Research Square

Preprints are preliminary reports that have not undergone peer review.
They should not be considered conclusive, used to inform clinical practice,
or referenced by the media as validated information.

Graphene-oxide modified TiO2 composite thin films for improved catalytic H2 evolution in NaBH4 hydrolysis and dye removal under UV illumination

Daniyal Ramazanov
Institute of Functional Materials
Imanzhussip Serkul
Nazarbayev University
Timur Sh. Atabaev
timur.atabaev@nu.edu.kz

Nazarbayev University

Research Article

Keywords: Graphene oxide, TiO2 thin films, photocatalytic dye removal, H2 evolution, NaBH4 hydrolysis

Posted Date: November 10th, 2026

DOI: https://doi.org/10.21203/rs.3.rs-11434415/v1

License: This work is licensed under a Creative Commons Attribution 4.0 International License.
Read Full License

Additional Declarations: No competing interests reported.

Graphene-oxide modified TiO_2 composite thin films for improved catalytic H_2 evolution in $NaBH_4$ hydrolysis and dye removal under UV illumination

Daniyal Ramazanov[1,#], Imanzhussip Serkul[2,#], Timur Sh. Atabaev[2,*]

[1] Institute of Functional Materials, Astana, Kazakhstan

[2] Department of Chemistry, Nazarbayev University, Astana, Kazakhstan

[#] - equal contribution

Corresponding author: timur.atabaev@nu.edu.kz

Abstract

This study reports the fabrication of graphene oxide (GO)-modified TiO_2 thin films with enhanced catalytic performance for H_2 evolution via $NaBH_4$ hydrolysis and photocatalytic methylene blue (MB) dye removal under UV irradiation. Among the investigated GO concentrations, the sample containing 100 μg of GO per 1 mL of TiO_2 slurry paste (TiO_2-100) exhibited the best performance in both processes. Specifically, MB removal increased by approximately 14%, while the hydrogen evolution rate improved by approximately 27.3%. The enhanced MB removal can be associated with enhanced electron transfer and suppressed charge recombination in TiO_2-100, while the enhanced H_2 evolution may be associated with changes in surface chemistry and improved interfacial interactions between the catalyst and aqueous reactants. The obtained results demonstrate the good potential of GO-modified TiO_2 thin films as low-cost catalysts for environmental remediation and hydrogen generation applications.

Keywords: Graphene oxide, TiO_2 thin films, photocatalytic dye removal, H_2 evolution, $NaBH_4$ hydrolysis

1 Introduction

Photocatalytic removal of pollutants using low-cost metal oxide semiconductors has attracted growing interest as a promising approach to addressing water pollution [1, 2]. Ideal photocatalysts should combine following features: low cost, high structural stability, efficient light activation, and the ability to generate reactive species for pollutant removal. Among various metal oxide semiconductors, TiO_2 is particularly attractive owing to its chemical stability and favorable

photocatalytic properties. As an n-type semiconductor with a wide band gap of approximately 3.2 eV, TiO_2 can generate reactive species under UV irradiation [3]. However, the recovery and reuse of dispersed TiO_2 nanostructures after water treatment can be challenging, potentially leading to secondary contamination. Using TiO_2 nanostructures in thin-film architectures offers a practical solution, enabling photocatalytic pollutant removal while facilitating reuse of photocatalytic film. Furthermore, low-cost UV LED sources, potentially powered by renewable energy, could provide an energy-efficient means of activating TiO_2-based photocatalytic films.

For photocatalytic films, reaction kinetics are generally expected to be slower than those of dispersed nanostructures. Therefore, TiO_2-based photocatalytic films are often combined with 2D materials, such as reduced graphene oxide (rGO), or graphene oxide (GO), to improve conductivity and facilitate charge separation. For example, electrochemically grown TiO_2-GO films increased the Reactive Yellow 145 dye degradation rate to approximately 77.8% compared with bare TiO_2 films [4]. Another report suggested that degradation rate of methylene blue (MB) dye with GO-TiO_2 film was higher to ~ 14.7% as compared to bare TiO_2 film [5]. Hence, these studies highlight the potential of 2D materials to enhance the degradation kinetics of organic pollutants in water using TiO_2-based photocatalytic films.

On the other hand, the potential of 2D material-modified TiO_2 thin films for catalytic hydrogen evolution during $NaBH_4$ hydrolysis remains unexplored, with most reported catalysts employed in powder form [6-8]. Therefore, this study focuses on optimizing the GO concentration in mesoscopic TiO_2 films for photocatalytic MB dye removal and catalytic H_2 evolution via $NaBH_4$ hydrolysis.

2 Experimental section

2.1 Materials and synthesis of films

High grade reagents were purchased from Merck and used as received. TiO_2-based slurry pastes containing different GO concentrations were prepared according to our previous report [9], while bare TiO_2 paste served as a reference. The pastes were labeled according to GO concentrations and deposited onto pre-cleaned glass substrates (26 × 15 mm) using a Spin-1200T spin coater (Midas System Co., Ltd.) at 2000 rpm for 20 s. The as-deposited films were dried under ambient

air conditions for 2 hours, followed by annealing at 500 °C (5°C/min heating rate) for 1 hour in a tube furnace under vacuum conditions to prevent GO burning.

2.2 Instruments

The surface morphology of the prepared samples was examined using a ZEISS Crossbeam 540 field-emission scanning electron microscope (FESEM). X-ray diffraction (XRD) was performed using the Smartlab Rigaku system with Cu Ka radiation (λ = 1.54056 Å). A LabRam Evolution system (Horiba Ltd.) was employed to perform the Raman analysis of the samples. X-ray photoelectron spectroscopy (XPS) analysis was performed using an Omicron MultiProbe X-ray photoelectron spectrometer.

Photocatalytic MB removal was evaluated using 10 mL of an aqueous MB solution (10 ppm) in a quartz vial. The film-coated glass substrate was immersed in the solution, and the vial was irradiated with a UV lamp (365 nm, 190 mW/cm^2). At predetermined time intervals, aliquots of the solution were withdrawn and analyzed using a Genesys 50 UV-Vis spectrophotometer. After each measurement, the solution was returned to the quartz vial to continue the photocatalytic experiment. All experiments were performed in triplicate to ensure the reproducibility of the results.

For H_2 evolution experiments, the film-coated glass substrate was immersed in an aqueous solution containing 50 mg of $NaBH_4$ in 30 mL of deionized water. The purity of the evolved H_2 was verified using an industrial multigas analyzer (S360), while the amount of H_2 generated was determined using the water displacement method. All experiments were performed in duplicate

3 Results and Discussion

In the first step, MB removal was evaluated over the first 20 min as a function of GO concentration in the TiO_2 films. As shown in Figure 1, the incorporation of GO flakes enhanced the photocatalytic removal of MB. Bare MB dye and bare TiO_2 thin films were also used as reference samples. One can observe that MB removal in first 20 min without any catalyst was found to be ~ 8.2 %. In the presence of bare TiO_2, the MB removal was increased to ~ 9.05%. However, samples with GO showed higher removal rate, especially for TiO_2-100 sample, which showed the best

photocatalytic MB removal of ~ 10.3 %. Further increase in GO content not significantly enhanced the photocatalytic MB removal, hence, TiO_2-100 sample was found to be the optimal one and used further for experiments.

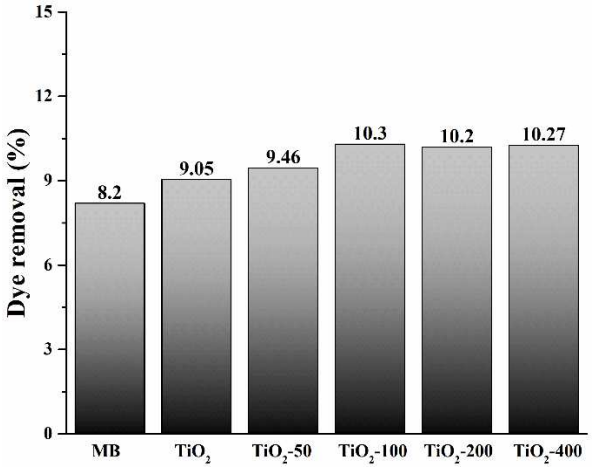


Figure 1. Photocatalytic MB removal comparison with and without GO-TiO_2 thin films at first 20 min.

Next, kinetics of MB removal with bare MB solution, bare TiO_2, and TiO_2-100 sample were monitored. Figure 2 shows that MB removal in the absence of a catalyst plateaued after the first 20 min, with no substantial further increase. In contrast, MB removal steadily increased over time in the presence of bare TiO_2 and TiO_2-100 films, with the latter exhibiting slightly higher photocatalytic activity. This trend was further supported by the apparent degradation rate constants, with the catalyst-free MB solution showing the lowest value (k_a = 0.0013 min^{-1}). The apparent degradation rate constants of bare TiO_2 and TiO_2-100 were 3.31 (k_a = 0.0043 min^{-1}) and 3.76 (k_a = 0.0049 min^{-1}) times higher, respectively, than that of the catalyst-free solution.

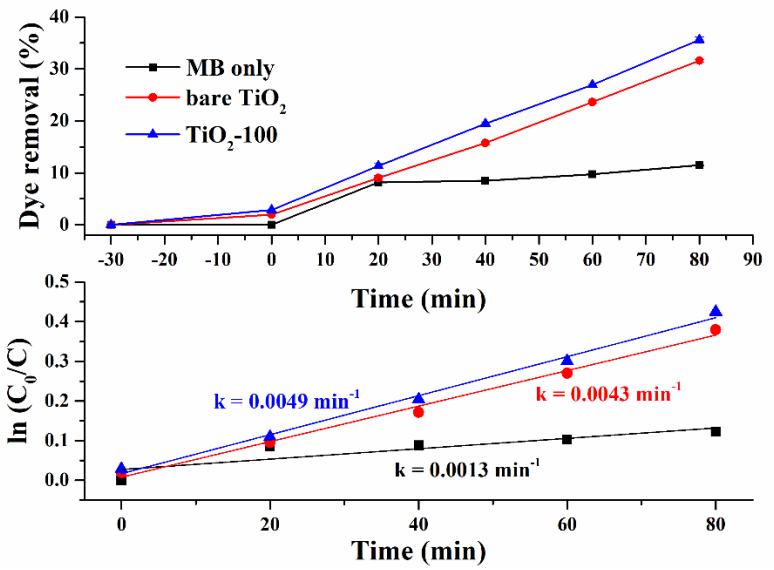


Figure 2. Photocatalytic MB removal kinetics of bare MB, bare TiO_2, and TiO_2-100 sample, and corresponding apparent degradation rate constants calculations.

For practical applications, MB removal with the optimal TiO_2-100 films was further evaluated at different pH values, in simulated saline water (3.5 wt.% NaCl), and in the presence of various scavengers to identify the reactive species involved. Figure 3 shows that MB removal decreased at lower pH, potentially due to competition between H^+ ions and positively charged MB molecules for adsorption sites on the film surface. In contrast, higher pH increased the availability of OH^- ions, which may contribute to the generation of additional reactive species and thereby enhance MB removal [10]. In NaCl solution, Cl^- ions can react with photogenerated holes, leading to the formation of chlorine radicals (Cl•) [11, 12]. As observed, the MB removal rate in the presence of NaCl was approximately three times higher than under pH=6 conditions. These results suggest that chloride-containing salts, which are commonly found in natural waters, may significantly enhance MB degradation.

Finally, scavengers were added to the MB solution to investigate the dye removal mechanism. In the absence of scavengers, MB removal reached 10.35% after first 20 min. The addition of IPA markedly reduced MB removal to 3.4%, suggesting that hydroxyl radicals (•OH) play a major role in MB degradation. In contrast, Na_2SO_4 increased MB removal to 19.3%, indicating that sulfate-derived reactive species, potentially including $SO_4^{\bullet -}$, may further promote degradation [13, 14].

The addition of BQ slightly decreased MB removal to 9.2%, suggesting that electron-mediated pathways may contribute to the process but are not dominant.

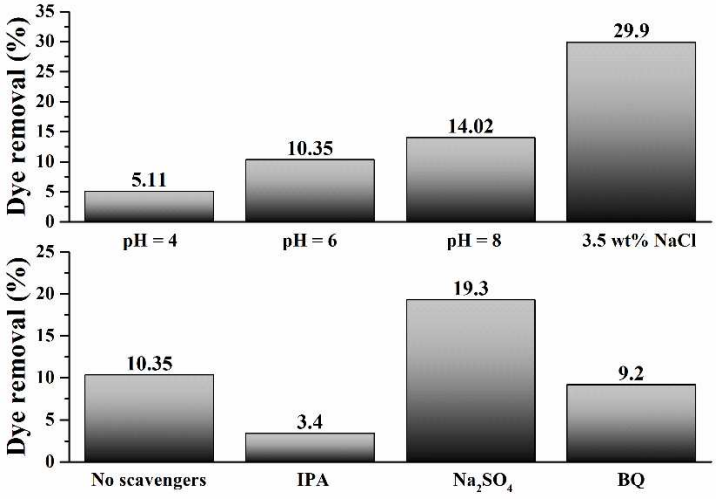


Figure 3. Photocatalytic MB removal with TiO_2-100 film at different pH values, in simulated saline water (3.5 wt.% NaCl), and in the presence of various scavengers.

In the next step, the prepared films were evaluated for catalytic H_2 evolution in $NaBH_4$ hydrolysis reactions. Figure 4 shows the hydrogen volume generated over 30 min, comparing uncatalyzed $NaBH_4$ with bare TiO_2 and various GO-TiO_2 thin films. During the initial 10 min, the thin films showed minimal differentiation, although all catalytic films outperformed the uncatalyzed $NaBH_4$ hydrolysis. The varied GO loadings produced similar hydrogen evolution volumes, ranging from ~ 4.5 to 5.0 mL. However, clear performance differences emerged at the 20-minute mark, where the TiO_2-100 film took a noticeable lead by generating 12.1 mL of hydrogen, outperforming both bare TiO_2 (10.45 mL) and uncatalyzed $NaBH_4$ hydrolysis (8.3 mL). By the final 30-minute measurement, the TiO_2-100 thin film achieved the highest overall hydrogen volume at 18.2 mL. This demonstrates that the TiO_2-100 film represents the optimal composite, in which the balance between exposed TiO_2 active sites and the GO network is maximized to facilitate high H_2 generation. The pronounced decline at higher GO concentrations suggests that excess GO can shield the active catalytic sites and hinder the overall hydrolysis reaction.

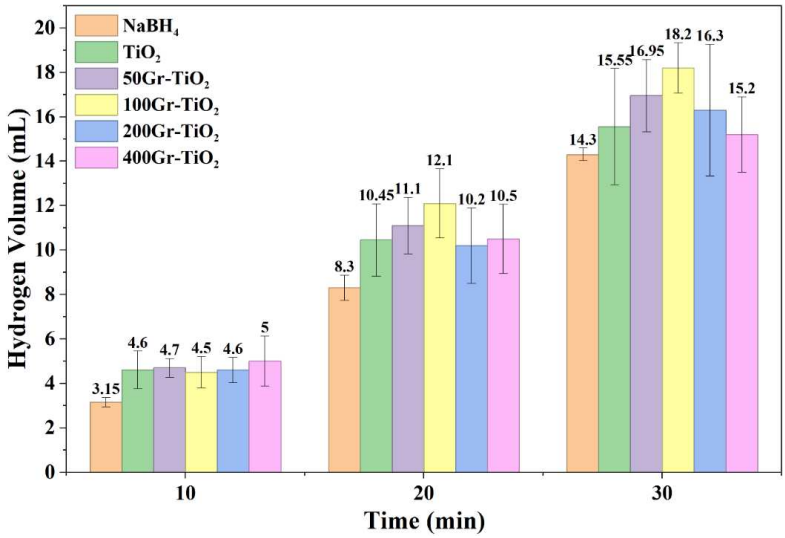


Figure 4. Uncatalyzed and catalyzed H_2 evolution during $NaBH_4$ hydrolysis

Next, the $NaBH_4$ hydrolysis was evaluated at various temperatures with bare $NaBH_4$ and optimal TiO_2-100 films. Figure 5 shows that H_2 evolution increased with temperature for both systems. Enhancements in H_2 evolution (~23-28%) were observed at all temperatures, demonstrating that TiO_2-100 consistently promotes the hydrolysis reaction.

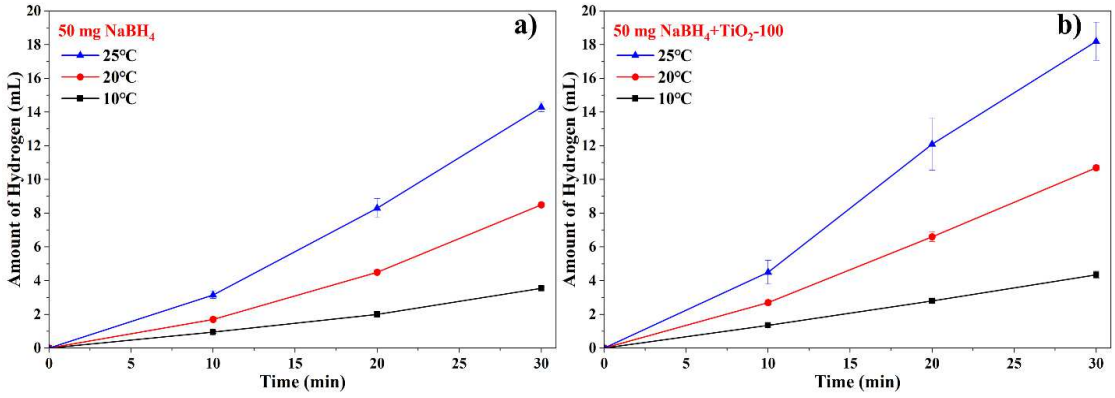


Figure 5. Uncatalyzed and TiO_2-100 catalyzed H_2 evolution during $NaBH_4$ hydrolysis at different temperatures.

The morphological and structural differences between the bare TiO_2 and optimal TiO_2-100 films were further assessed using FESEM, XRD, Raman, and XPS. Figure 6 shows that the TiO_2 and

TiO_2-100 films exhibit very similar morphology - a porous network of TiO_2 nanoparticles assembled into a film. At this low loading concentration, the GO flakes are likely well dispersed within the TiO_2 matrix, as no GO flakes are observed on the film surface.

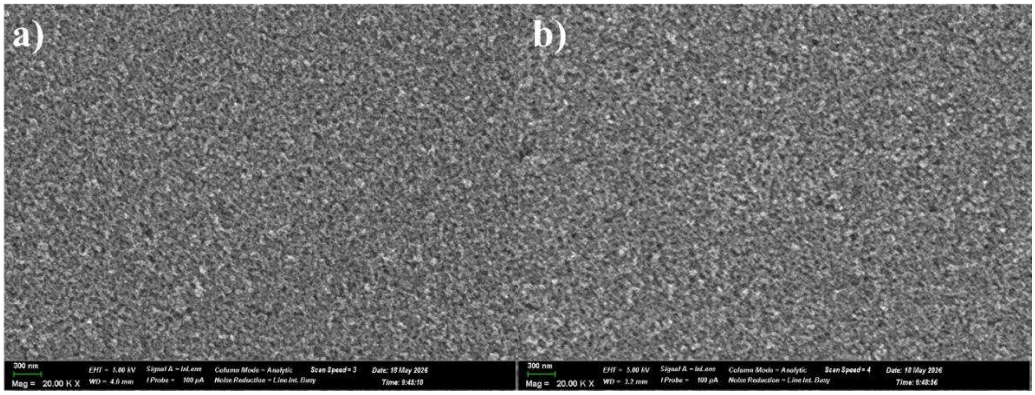


Figure 6. FESEM images of (a) TiO_2 and (b) TiO_2-100 films. Scale bar – 300 nm.

The XRD patterns of the bare TiO_2 and optimal TiO_2-100 films, together with the reference pattern, are depicted in Figure 7. Both samples match the anatase TiO_2 reference pattern, with the main reflections appearing at approximately 25.3° (101), 37.8° (004), 48.0° (200), 53.9° (105), 55.1° (211), and 62.7° (204), along with some weaker reflections at higher angles [3, 15]. The reflection peak positions of the two films are essentially identical, and no GO or graphite (002) reflection near 26.5° is detected, which is typical of low GO loadings. Notably, no other TiO_2 phases are detected, suggesting that both samples are in anatase phase.

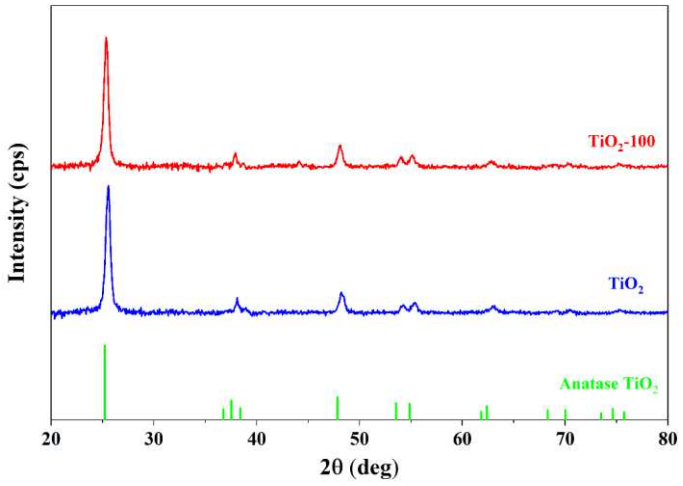


Figure 7. XRD patterns of bare TiO_2 and TiO_2-100 films.

Raman analysis of the bare TiO_2 and TiO_2-100 films was performed to confirm the successful incorporation of GO. Figure 8 shows that both samples exhibit similar peaks associated with the anatase TiO_2 structure, whereas the TiO_2-100 film displays two additional broad bands at ~1345 cm^{-1} (D) and ~1590 cm^{-1} (G) that are absent in bare TiO_2. The D-band appears because of lattice disorder and structural defects introduced by oxygen-containing epoxide and hydroxyl groups on the carbon basal plane, whereas the G-band is usually attributed to the in-plane stretching vibration of sp^2-hybridized C-C bonds characteristic of graphitic domains [5]. The appearance of these two characteristic peaks confirms the successful incorporation of the GO structure into the TiO_2 films. The D-band intensity is comparable to that of the G-band, with $I_D/I_G = 0.95$, and both bands are broad, indicating that a defective GO structure, rather than pristine graphene, exists within the TiO_2 films.

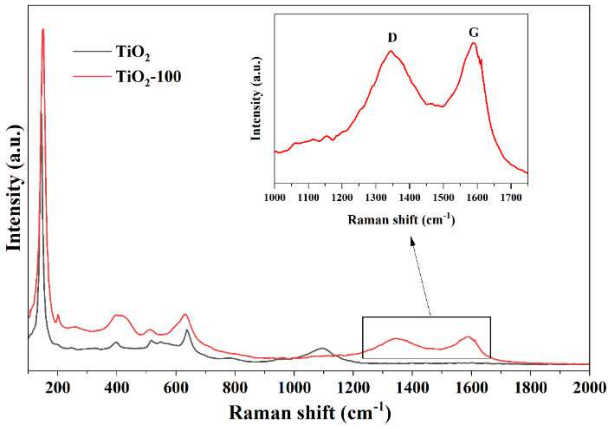


Figure 8. Raman spectra of bare TiO_2 and TiO_2-100 films.

Finally, the samples were characterized by high-resolution XPS. The Figure 9 compares the high-resolution C 1s, O 1s, and Ti 2p spectra of bare TiO_2 (a-c) and TiO_2-100 (d-f). The atomic percentages show only small differences between the samples: Ti decreases slightly from 30.72 to 30.10 at.%, while O increases from 66.12 to 66.27 at.% and C from 3.16 to 3.63 at.%. In the C 1s spectra, both samples exhibit a dominant component at 284.8 eV, assigned to C-C/C=C bonds, together with higher-binding-energy components attributed to C-O-C and O-C=O groups. For bare TiO_2, these components are located at 286.1 and 288.7 eV, respectively, whereas for TiO_2-100

they appear at 286.6 and 288.4 eV. The slightly higher carbon content of TiO_2-100 (3.63 at.% vs. 3.16 at.% for bare TiO_2) and the observed oxygen-containing carbon components are consistent with the presence of GO in the TiO_2-100 film. The O 1s spectra of both samples are dominated by the Ti-O component, located at 529.8 eV for bare TiO_2 and 529.6 eV for TiO_2-100. A higher-binding-energy contribution at approximately 531 eV is assigned to surface hydroxyl groups. The Ti 2p spectra show the characteristic Ti $2p_{3/2}$ and Ti $2p_{1/2}$ peaks at 458.6 and 464.2 eV for bare TiO_2, and 458.47 and 464.1 eV for TiO_2-100, respectively. These small binding-energy shifts indicate that the Ti chemical state remains broadly similar following GO modification, with no substantial change in the principal Ti-O bonding environment. Overall, the small increase in carbon content and the C 1s components associated with oxygen-containing carbon groups are consistent with GO incorporation, while the Ti 2p and O 1s spectra indicate that the TiO_2 framework is largely retained.

The beneficial effect of GO incorporation may be explained by two possible contributions: during photocatalysis, GO may promote charge separation and suppress electron-hole recombination, whereas the enhanced H_2 evolution during $NaBH_4$ hydrolysis may be related to changes in surface wettability, reactant adsorption, and the accessibility of catalytic sites.

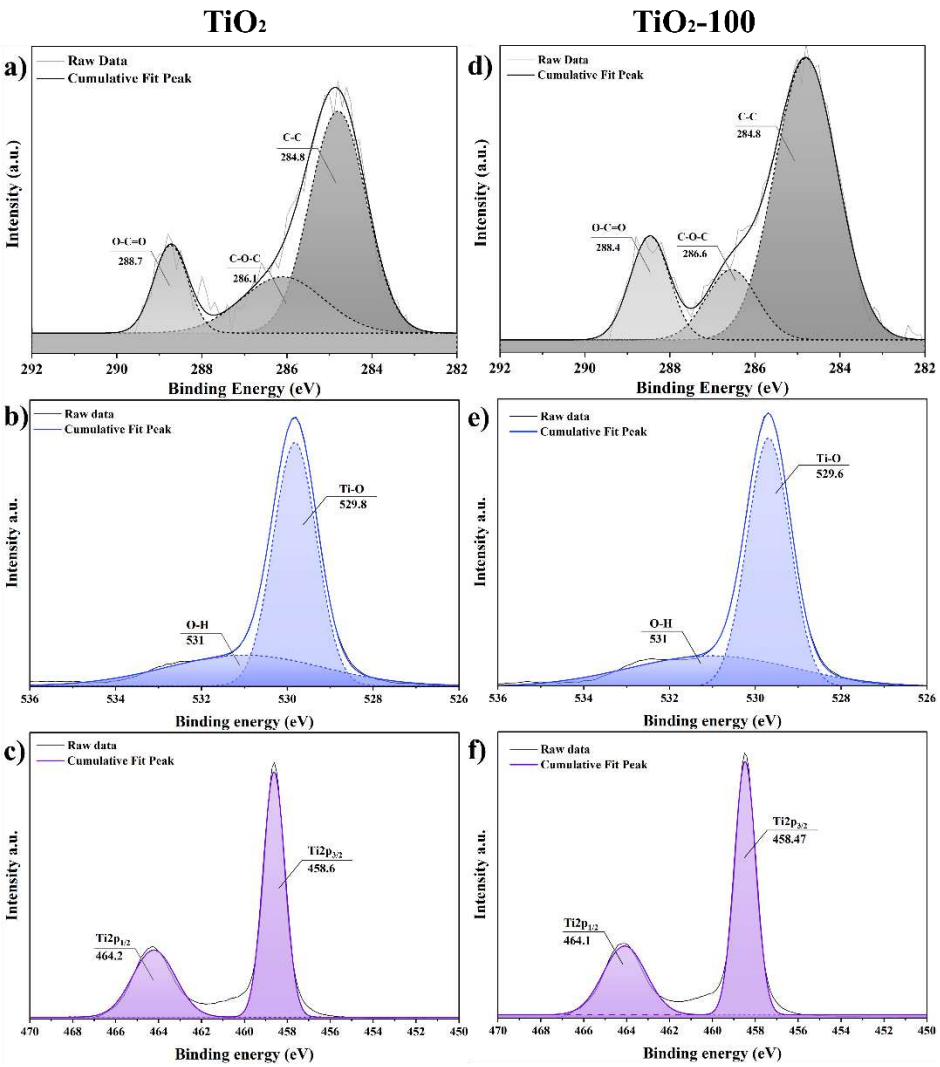


Figure 9. High resolution XPS analysis of C, Ti, and O elements of (a, b, c) TiO_2 and (d, e, f) TiO_2-100 films.

4 Conclusion

In this study, GO-modified mesoscopic TiO_2 films were investigated for MB photodegradation and H_2 evolution during $NaBH_4$ hydrolysis. The GO loading influenced the performance of the films, with TiO_2-100 exhibiting the most pronounced improvement among the tested compositions. Under UV irradiation, TiO_2-100 achieved approximately 14% higher MB removal than bare TiO_2, while its H_2 generation rate during $NaBH_4$ hydrolysis increased by 27.3%. High-resolution XPS showed that GO incorporation caused only minor changes in surface composition

and did not substantially alter the principal Ti-O chemical environment. The enhanced performance may therefore be associated with interfacial effects of GO, potentially including improved charge separation during photocatalysis and changes in surface wettability, reactant adsorption, or catalytic-site accessibility during $NaBH_4$ hydrolysis. These findings highlight the potential of GO-modified TiO_2 films as versatile catalysts for environmental remediation and hydrogen generation.

Author contributions

Daniyal Ramazanov: Data curation, formal analysis, investigation, methodology, writing - original draft. **Imanzhussip Serkul:** Data curation, formal analysis, investigation, methodology, writing - original draft. **Timur Sh. Atabaev:** Data curation, formal analysis, funding acquisition, investigation, methodology, writing - review and editing.

Funding

This research has been funded by the Committee of Science of the Ministry of Science and Higher Education of the Republic of Kazakhstan (Grant No. BR28712489).

Data availability

Data supporting the findings are available from the corresponding author upon reasonable request.

Declarations

Ethics approval and consent to participate

Not applicable. This article does not contain any studies with human participants or animals performed by any of the authors. This study did not involve human participants.

Consent for publication

Not applicable.

Competing interests

The authors declare no competing interests.

References

1. Al Miad A, Saikat SP, Alam MK, Hossain MS, Bahadur NM, Ahmed S. Metal oxide-based photocatalysts for the efficient degradation of organic pollutants for a sustainable environment: a review. Nanoscale Adv. 2024;6(19):4781–4803. https://doi.org/10.1039/d4na00517a

2. Leishangthem N, Das J, Singh NR, Singh NM. Multifunctional metal oxide photocatalysts for water purification: advances in organic pollutant degradation and antibacterial applications. Sustain Chem One World. 2025;8:100128. https://doi.org/10.1016/j.scowo.2025.100128

3. Rustembekkyzy K, Molkenova A, Kaikanov M, Atabaev TS. Deposition of inverse opal-like TiO_2 thin film with enhanced photoelectrochemical activity by a spin-coating combined with a dip-coating method. Nano Express. 2023;4:026001. https://doi.org/10.1088/2632-959X/acd131

4. Oliveira AG, Nascimento JP, Gorgulho HF, Martelli PB, Furtado CA, Figueiredo JL. Electrochemical synthesis of TiO_2/graphene oxide composite films for photocatalytic applications. J Alloys Compd. 2016;654:514-522 https://doi.org/10.1016/j.jallcom.2015.09.110

5. Vallejo W, Rueda A, Díaz-Uribe C, Grande C, Quintana P. Photocatalytic activity of graphene oxide–TiO_2 thin films sensitized by natural dyes extracted from Bactris guineensis. R Soc Open Sci. 2019;6(3):181824. https://doi.org/10.1098/rsos.181824

6. Arakelyan D, Abisheva D, Rustembekkyzy K, Kerim T, Atabaev TS. Hydrothermal synthesis of CuO flake-like structures for efficient degradation of model pollutant dye under solar light illumination and improved hydrogen evolution via catalytic $NaBH_4$ hydrolysis. JCIS Open. 2026;21:100169. https://doi.org/10.1016/j.jciso.2025.100169

7. Santos FL, Giroto AS, Torres JA, Oliveira AVPS, Santos VMFE, Nogueira AE. Hydrogen generation via $NaBH_4$ hydrolysis over cobalt-modified niobium oxide catalysts. Int J Hydrogen Energy. 2024;92:113–123. https://doi.org/10.1016/j.ijhydene.2024.10.236

8. Mandal P, Khandelwal K, Rana U, Sarkar PK, Sinhamahapatra A. Rate enhancement of $NaBH_4$ hydrolysis using light over graphitic carbon nitride-based catalyst. Int J Hydrogen Energy. 2026;236:155193. https://doi.org/10.1016/j.ijhydene.2026.155193

9. Khamkhash L, Em S, Molkenova A, Hwang YH, Atabaev TS. Crack-free and thickness-controllable deposition of TiO_2–rGO thin films for solar harnessing devices. Coatings. 2022;12(2):218. https://doi.org/10.3390/coatings12020218

10. Sen S, et al. Effect of pH on photocatalytic degradation of methylene blue in water by facile hydrothermally grown TiO_2 nanoparticles under natural sunlight. JCIS Open. 2025;19:100150. https://doi.org/10.1016/j.jciso.2025.100150

11. Zhang HC, Ma J. Enhanced radical generation in an ultraviolet/chlorine system through the addition of TiO_2. Environ Sci Technol. 2021;55(17):11612–11623. https://doi.org/10.1021/acs.est.0c08785

12. Yang F, Tian W, Bian Y, Liu Y, Li Z, Guo W, Zhao Y, Chen F, Wang L, Zhang X. Chlorine radicals in the environment: A critical review of reactivity, formation, and reaction across aqueous and atmospheric compartments. Environ Technol Innov. 2026;43:105042. https://doi.org/10.1016/j.eti.2026.105042

13. Babaei AA, Golshan M, Kakavandi B. A heterogeneous photocatalytic sulfate radical-based oxidation process for efficient degradation of 4-chlorophenol using TiO_2 anchored on Fe oxides@carbon. Process Saf Environ Prot. 2021;149:35–47. https://doi.org/10.1016/j.psep.2020.10.028

14. Piątkowska A, Szymański K, Mozia S. Effect of sulfur on the solar light photoactivity of TiO_2-based photocatalysts. Chem Eng Res Des. 2023;195:721–731. https://doi.org/10.1016/j.cherd.2023.04.049

15. Rajawat A, Shekhawat A, Maurya M, et al. Biogenically engineered magnetic Fe_2O_3 coupled with anatase TiO_2 nanomaterials for effective photocatalytic study. Discov. Chem. 2026;3:284. https://doi.org/10.1007/s44371-026-00740-3